Nowaczyk, N., Knies, J. (2000): Magnetostratigraphic results from the eastern Arctic Ocean: AMS 14C ages and relative palaeointensity data of the Mono Lake and Laschamp geomagnetic reversal excursions. - Geophysical Journal International, 140, 1, pp. 185—197.

DOI: https://doi.org/10.1046/j.1365-246x.2000.00001.x

Geophys. J. Int. (2000) **140,** 185–197

Magnetostratigraphic results from the eastern Arctic Ocean: AMS ^{14}C ages and relative palaeointensity data of the Mono Lake and Laschamp geomagnetic reversal excursions

Norbert R. Nowaczyk[1] and Jochen Knies[2]

[1] *GeoForschungsZentrum Potsdam, Projektbereich* 3.3 *'Sedimente und Beckenbildung', Laboratory for Palaeo- and Rock Magnetism, Telegrafenberg,* 14473 *Potsdam, Germany. E-mail: nowa@gfz-potsdam.de*

[2] *Alfred-Wegener-Institute for Polar and Marine Research, Columbusstrasse,* 27568 *Bremerhaven, Germany*

Accepted 1999 August 18. Received 1999 July 23; in original form 1999 February 4

SUMMARY

A new high-resolution magnetostratigraphic record from the eastern Arctic Ocean has yielded further evidence for the existence of the Laschamp excursion (37–35 ka), the Mono Lake excursion (27–25.5 ka) and possibly another very short excursion (22 ka) inferred from steep negative inclinations. Ages are based on nine AMS (accelerator mass spectrometry) ^{14}C dates, oxygen isotope stratigraphy and correlation with ODP site 983. Estimates of relative palaeointensity variations for the time interval from 80 to 10 ka have revealed that the documented geomagnetic excursions are linked to large fluctuations of the relative palaeointensity. The lowest values were obtained for the two excursions and the normal–reversed (N–R) and reversed–normal (R–N) transitions of the Laschamp polarity excursion, which itself is characterized by a slight increase of relative palaeointensity during its reversed state. The results are in general agreement with palaeointensity studies from other regions, indicating that these fluctuations could be global phenomena and that the geomagnetic field of the Brunhes Chron was very variable in amplitude as well as in geometry. The new result is one of the rare records comprising large directional as well as large relative palaeointensity variations.

Key words: Arctic Ocean, Brunhes Chron, geomagnetic reversals, Laschamp excursion, magnetostratigraphy, Mono Lake excursion.

INTRODUCTION

Sediments from northern high latitudes turned out to be a good recording material of short-term geomagnetic field variations throughout the Brunhes Chron; that is, excursions, as expressed by steep negative inclinations (Løvlie *et al.* 1986; Bleil & Gard 1989; Nowaczyk & Baumann 1992; Nowaczyk *et al.* 1994; Schneider *et al.* 1996; Nowaczyk & Antonow 1997; Nowaczyk & Frederichs 1999). Recent syntheses concerning the ages and durations of these high-frequency features of the geomagnetic field were published by Løvlie (1989a,b), Nowaczyk *et al.* (1994), Langereis *et al.* (1997), Nowaczyk & Antonow (1997), Lund *et al.* (1998), and Gubbins (1999).

Assuming that the degree of alignment of the magnetic particles during deposition is proportional to the ambient magnetic field, numerous studies have been performed during the last decade to reconstruct the palaeointensity variations of the geomagnetic field (e.g. Tauxe & Valet 1989; Tauxe 1993; Channell *et al.* 1997; Roberts *et al.* 1997; Guyodo & Valet 1999). A relative palaeointensity record from the Equatorial Pacific Ocean showed pronounced minima that were related tentatively by Valet & Meynadier (1993) to the short-term geomagnetic excursions within the Brunhes Chron as listed by Champion *et al.* (1988), a fairly obsolete compilation (see Langereis *et al.* 1997). Nevertheless, in the Pacific Ocean data set itself, no evidence for non-normal polarity directions was found directly. Until now, only a few studies focusing on relative palaeointensity variations have revealed evidence for both low palaeointensities and directional variations in terms of polarity excursions (Weeks *et al.* 1995; Schneider *et al.* 1996; Channell *et al.* 1997; Nowaczyk 1997; Roberts *et al.* 1997; Völker *et al.* 1998). In this paper we present a new, and for polar regions exceptionally well-dated, high-resolution palaeointensity record from 81.5°N for the time interval 10–80 ka including the Laschamp polarity excursion (Bonhommet & Babkine 1967; Gillot *et al.* 1979) at 37–35 ka, the Mono Lake excursion (Denham & Cox 1971; Liddicoat & Coe 1979) at 27–25.5 ka, and possibly a short excursion at around 22 ka.

MATERIALS AND METHODS

Sediment core PS 2138–1 SL, 635 cm long, was recovered from northeast of Svalbard at 81.5°N, 30.6°E (Fig. 1) with the help

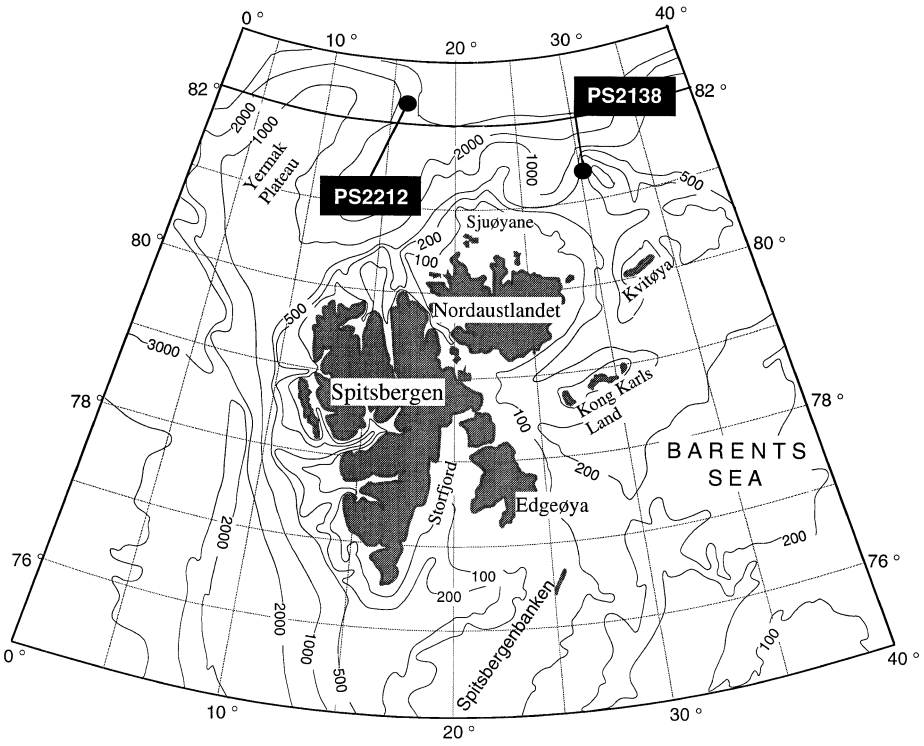

Figure 1. Locations of cores PS 2138–1 SL and PS 2212–3 KAL discussed in this study.

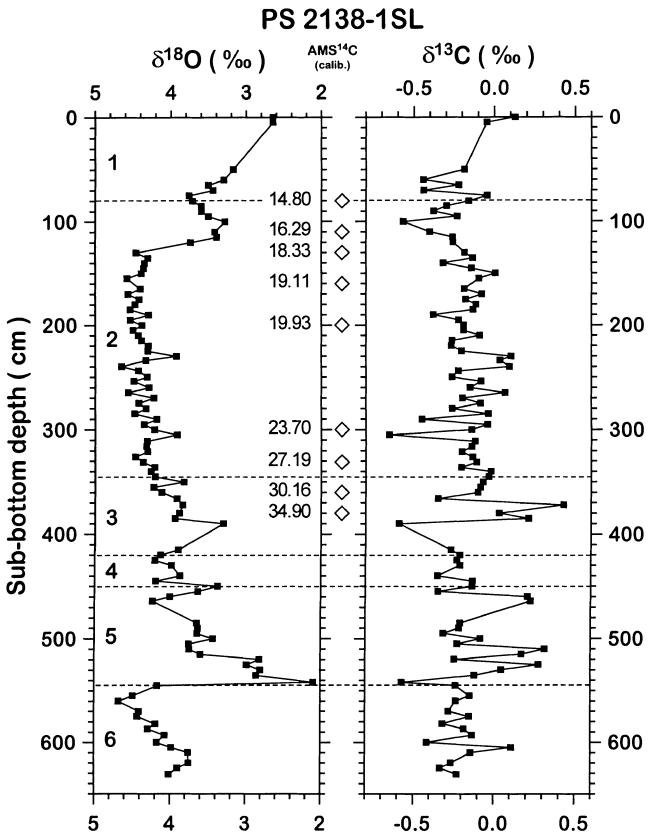

Figure 2. Stable oxygen (δ^{18}O) and carbon (δ^{13}C) isotope stratigraphy of core PS 2138–1 SL. Numbers to the left of the open diamonds indicate calibrated AMS ^{14}C ages. Dashed lines mark boundaries of oxygen isotope stages that are indicated by numbers from 1 to 6 in the left plot.

Table 1. Age model of core PS 2138–1 SL. Note that oxygen isotope stage boundaries 1/2 (event 2.0) and 2/3 (event 3.0) were recalculated to calibrated AMS ^{14}C ages. Calendar ages were calculated using the CALIB 3.0 program of Stuiver & Reimer (1993).

Depth (cm)	Ages (ka)			
	AMS ^{14}C $\pm$ error	AMS ^{14}C, calib.	δ^{18}O	Event
75			13.89	2.0
80	12.60 + 140/−130	14.80		
110	13.59 + 80/−80	16.29		
130	15.41 + 130/−130	18.33		
160	16.23 + 210/−210	19.11		
200	16.88 + 130/−130	20.57		
300	20.04 + 330/−320	23.70		
331	23.10 + 240/−240	27.19		
345			28.18	3.0
360	25.80 + 280/−270	30.16		
380	34.90 + 1570/−1310	(34.9)		
415			55.98	3.3.1
420			59.00	4.0
450			74.00	5.0
460			79.92	5.1
500			103.59	5.3
510			109.50	5.4
545			130.00	6.0
560			135.00	6.2
610			142.00	6.3
631			145.00	

of *R/V Polarstern* from a water depth of 995 m using a gravity corer (Schwerelot, SL) with a diameter of 12 cm. The recovered sediments are composed of greyish/greenish to dark brown as well as dark grey silty clays. Some distinct layers are of reddish

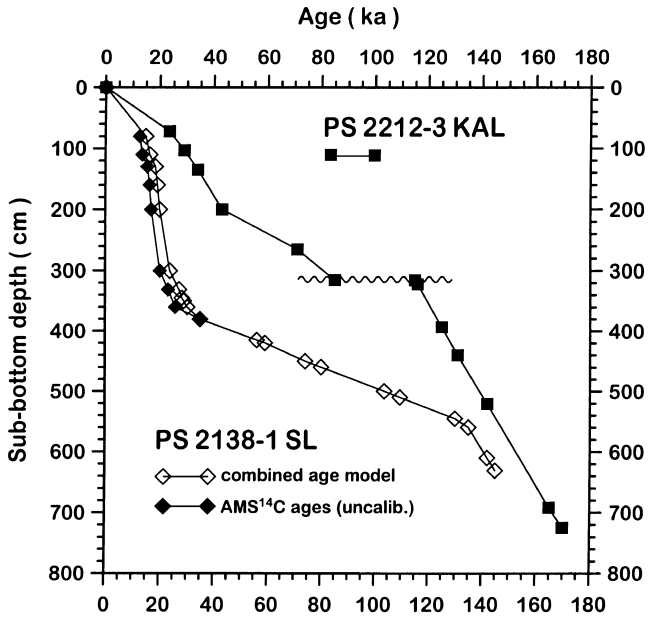

Figure 3. Age models of core PS 2138–1 SL (see also Table 1) and core PS 2212–3 KAL (Nowaczyk *et al.* 1994). The wavy line indicates a hiatus in core PS 2212–3 KAL.

and light yellowish colour. Carbonate content ranges from 3 to 20 per cent. Planktonic foraminifera *Neogloboquadrina pachyderma* sin. from the >63 μm fraction were used to perform stable oxygen and carbon isotope measurements. Several samples were also chosen for accelerator mass spectrometry (AMS) ^{14}C dating. Calendar years, referred to as 'calibrated ages', were calculated using the program CALIB 3.0 of Stuiver & Reimer (1993). An extended second-order fit from Bard *et al.* (1992) was used for calculating calendar ages >18 kyr. More detailed descriptions of preparation, measuring techniques and results from sedimentological as well as geochemical analyses of the sediments are given in Knies (1999).

Magnetic susceptibility was scanned at the split surface of the core in steps of 2.5 mm using a Bartington MS2E/1 sensor following a procedure analogous to that described by Nowaczyk & Antonow (1997) for the MS2F sensor. The half-width of the bell-shaped sensor characteristics along the core axis is only 4 mm, yielding a spatial resolution three times better than that of the MS2F sensor with a half-width of 12 mm. Moreover, the MS2E/1 sensor integrates more perpendicular to than along the core axis, yielding a higher-amplitude sensitivity, about twice as good as the MS2F sensor.

The core was sampled every 2–3 cm with 6.2 cm^3 cubic plastic boxes, yielding a total of 258 samples. Measurements

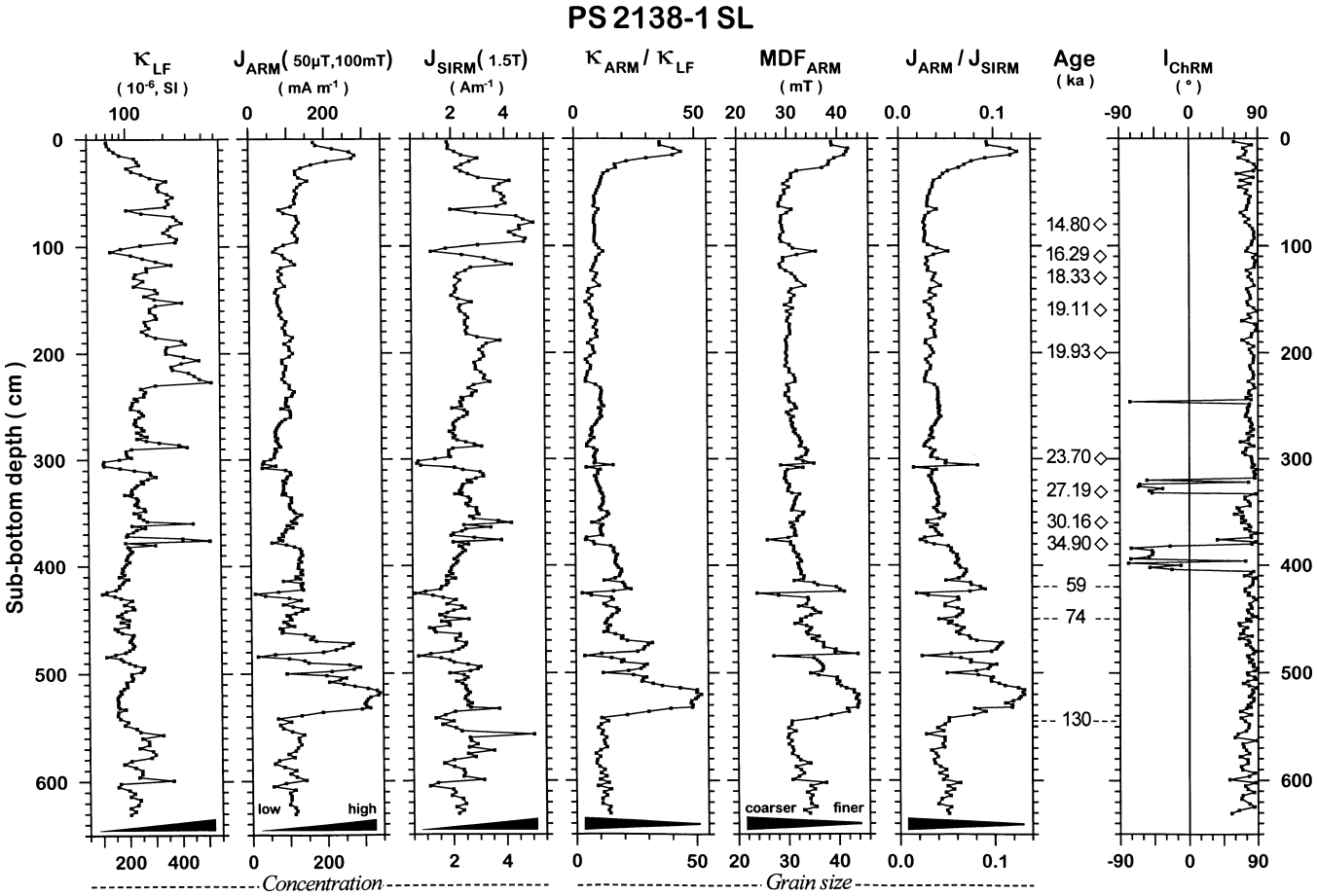

Figure 4. Results of concentration- and grain-size-related rock magnetic investigations, ages (open diamonds: calibrated AMS ^{14}C ages; dashed lines: oxygen isotope stage boundaries) and inclination of characteristic remanent magnetization (I_{ChRM}) from PS 2138–1 SL.

of the low-field bulk susceptibility, κ_{LF}, of the palaeomagnetic samples were performed with an AGICO Kappabridge KLY-3S. Measurements and demagnetization of the natural remanent magnetization (NRM) and anhysteretic remanent magnetization (ARM) were performed with a fully automated 2G Enterprises DC-SQUID 755 SRM long-core system with an in-line triaxial alternating field (AF) demagnetizer. ARMs were produced along the samples' positive *z*-axes with a 0.05 mT static field and 100 mT AF amplitude using a separate 2G Enterprises 600 single-axis demagnetizer including an ARM coil (maximum static field 1 mT). Isothermal remanent magnetizations (IRM) were imprinted with a 2G Enterprises 660 pulse magnetizer and measured with a Molyneux MiniSpin fluxgate magnetometer (noise level 0.2×10^{-3} Am^{-1} for 6.2 cm^3 samples), because IRMs often exceed the sensitivity range of the cryogenic magnetometer. IRM intensities were acquired in a direct field of 1.5 T and are referred to as saturation IRM (SIRM).

According to the method of Nowaczyk (1997), estimates of relative palaeointensity variations were calculated by dividing NRM intensities after 50 mT AF demagnetization by

(1) the low-field magnetic susceptibility κ_{LF},
(2) the SIRM intensity, and
(3) ARM intensities, also after demagnetization with 50 mT,

and then normalizing each curve to its average.

RESULTS

Chronology

Results from stable oxygen and carbon isotopes as well as AMS ^{14}C dating from core PS 2138–1 SL are shown in Fig. 2. The data are quite exceptional since northern high-latitude sediments are commonly barren of biogenic relicts so that often only incomplete or no isotope records can be obtained. The tie-points of the resulting age model are listed in Table 1 and plotted in Fig. 3, together with the age model of core PS 2212–3 KAL (Nowaczyk *et al.* 1994). This core was taken some 200 km to the west of site 2138 and will be used for correlation. According to the age model provided by stable isotope and AMS ^{14}C dating, core PS 2138–1 SL has a maximum age of about 145 kyr. Mean sedimentation rates are highest, about 18 cm kyr^{-1}, in the time interval from approximately 15–30 ka, and lowest, less than 2 cm kyr^{-1}, between 30 and 130 ka (Fig. 2). During the Holocene and oxygen isotope stage (OIS) 6, sedimentation rates are in the range of about 5 cm kyr^{-1}.

Rock magnetism

The rock magnetic parameters derived from core PS 2138–1 SL, together with the inclination of the characteristic remanent magnetization (I_{CHRM}), discussed below, are shown in Fig. 4. Regarding the parameters related to the concentration of magnetic minerals, κ_{LF}, ARM and SIRM (Fig. 4, left), it appears that the correlation of susceptibility with SIRM yields a fairly linear trend (Fig. 5a), whereas the correlation of susceptibility with ARM is more complex. Only a subset of the samples yields a linear trend; the rest show a greater scatter (Fig. 5b). Obviously, the deviations in the concentration parameters are caused by grain-size variations, since the ARM is

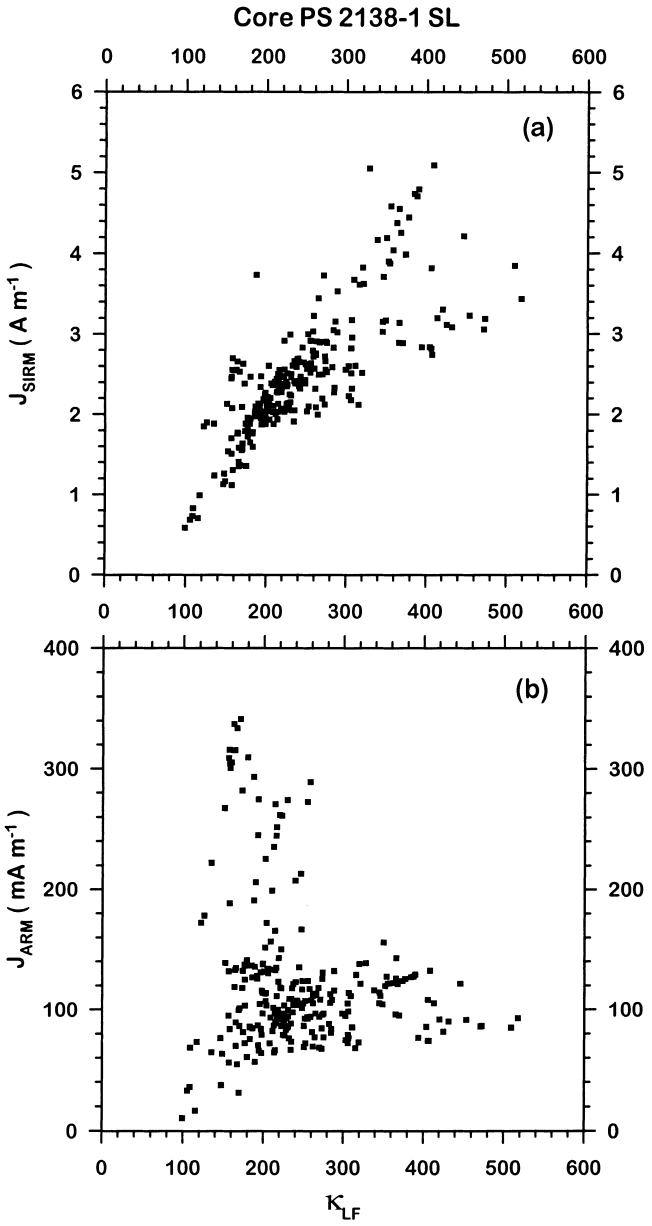

Figure 5. Intensity of (a) J_{SIRM} and (b) J_{ARM} versus low-field magnetic susceptibility, κ_{LF}.

mainly carried by smaller (single domain to pseudo-single domain) magnetic particles, whereas κ_{LF} and SIRM are linked more to larger (multidomain) particles. Therefore, ratios of κ_{ARM}/κ_{LF}, where κ_{ARM} is ARM divided by the amplitude of the applied static field during its acquisition (King *et al.* 1982; Hall & King 1989; Bloemendal *et al.* 1992), and J_{ARM}/J_{SIRM} can be used, in a first approximation, as indicators of relative grain-size changes with high (low) values indicating smaller (larger) particles. Within PS 2138–1 SL, in the uppermost 30 cm (late Holocene) and in the interval from about 465 cm to 535 cm (equivalent to stage 5), these ratios point to significantly smaller particles. This observation is supported by the median destructive field of the ARM (MDF_{ARM}), since smaller particles are more resistant to AF demagnetization than larger particles.

In general, except for the two intervals mentioned above, the rock magnetic parameters do not vary too much and fit the required conditions of Tauxe (1993) for palaeointensity estimates. Samples with reversed inclinations fall within the quite homogeneous section between 30 and 465 cm and are therefore interpreted as records of geomagnetic field variations, as discussed in the following section.

Palaeomagnetism

The results of three different palaeointensity estimates are shown in Fig. 6. Because of the strongly varying grain sizes of the magnetic particles, samples from above 35 cm, and from 495 to 540 cm yielded very different results (Fig. 6a). In addition, ARM intensities between 460 and 540 cm were significantly higher (Fig. 6c). To reduce concentration as well as grain-size variations to a minimum, the three palaeointensity estimates were normalized to their average for only the interval 35–460 cm. The recalculated estimates showed a better congruence (Fig. 6b). In the lowermost part of the core, from 545 to 630 cm, the palaeointensity estimates also showed a good match, and ARM intensity did not vary much; however, this core section is too short for any interpretation. In the following discussion the term 'relative palaeointensity' refers to the ratio $PJ = J_{NRM}(50\ mT)/J_{ARM}(50\ mT)$ smoothed with a three-point triangular window $[PJ_S(n) = 0.25\ PJ(n-1) + 0.5\ PJ(n) + 0.25\ PJ(n+1)$, where PJ_S is smoothed $PJ]$. A plot of J_{ARM} versus $J_{NRM}(50\ mT)/J_{ARM}(50\ mT)$ proves that the relative palaeointensity estimate is not biased by environmental changes, for example concentration variations due to climatic cycles (Fig. 7).

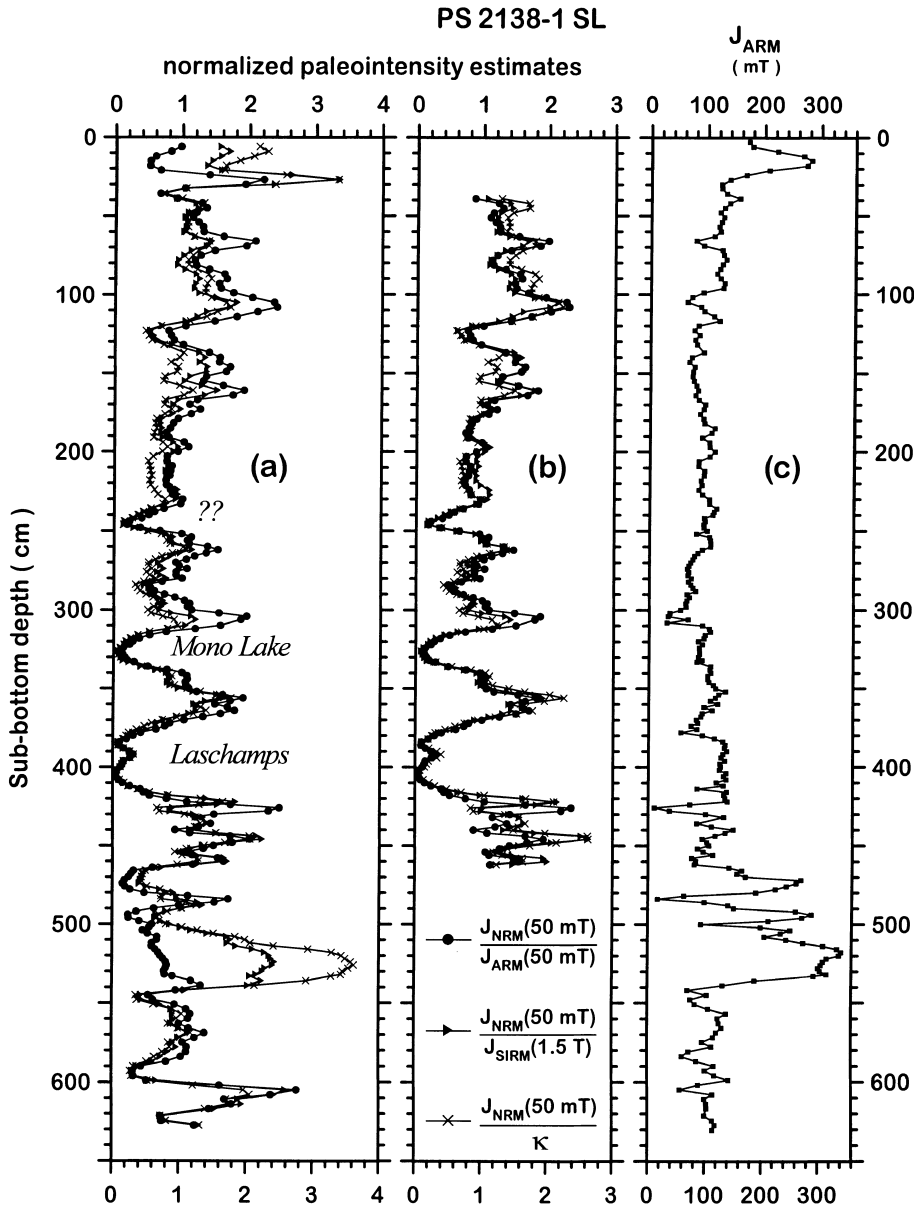

Figure 6. Palaeointensity estimates, as indicated by the legend, after normalization to the average for core PS 2138–1 SL. The three curves exhibit large differences above 35 cm and between 495 and 540 cm (a). Palaeointensity normalization was recalculated for the interval 35–460 cm only (b), because the ARM intensities (J_{ARM}) show minimum scatter in this interval (c). The results now agree better. All records were smoothed with a three-point running average (triangular window, see text).

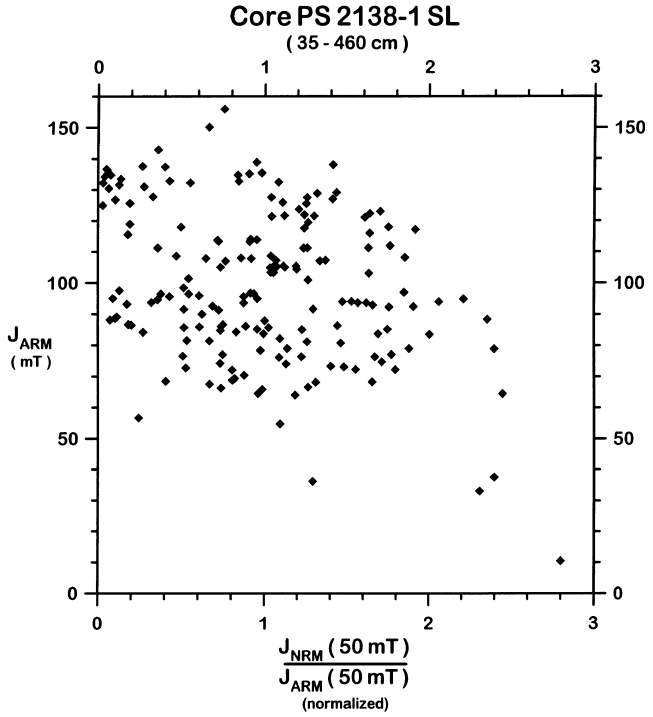

Figure 7. ARM intensity (J_{ARM}) versus relative palaeointensity approximated by the ratio $J_{NRM}(50\,mT)/J_{ARM}(50\,mT)$ derived from core PS 2138–1 SL for the depth interval 35–460 cm.

The characteristic remanent magnetizations (ChRM), based on principle component analysis (Kirschvink 1980) together with the median destructive fields of the NRM (MDF_{NRM}), the NRM intensities (J_{NRM}) and the results from high-resolution logging of magnetic susceptibility are shown in Fig. 8. The inclination of the mean direction is 86.1° ($\alpha_{95} = 1.6°$), very close to the expected dipole inclination of 85.7°. Nevertheless, in the equal-area projection, ChRM directions cluster mainly within a circular window with a radius of approximately 25° around their mean, resulting in an (apparently) large scatter of the ChRM declinations due to the high northern latitude of the coring site. ChRM declinations in Fig. 8 are corrected for their mean value as an approximation of the true North.

Two pronounced geomagnetic excursions (318–332 cm and 380–405 cm) are visible in the ChRM inclination. By means of the AMS ^{14}C ages, the two excursions can be unequivocally related to the Mono Lake excursion and the Laschamp excursion, respectively. Zijderveld plots of three successive samples from the Laschamp excursion (Fig. 9) show that the reversed high-coercivity directions are overprinted by a large normal-polarity (low-coercive) component. In this case the viscous component could be removed in fields of 20–25 mT (5th and 6th data points in Fig. 9). However, the overprint of other samples with a reversed ChRM inclination had to be removed with fields of up to 50 mT. Therefore, palaeointensity estimates are based on NRM intensities after treatment in 50 mT AF amplitude. Similarly to results from the Greenland Basin (Nowaczyk 1997), relative palaeointensity starts to decrease from relatively high values at about 60 ka. Reaching a pronounced intensity minimum between 56 and 35 ka, the field vector reverses polarity; this is followed by a slight recovery of the field strength during the reversed state of the Laschamp excursion (Fig. 10), a feature that is also present in the Greenland Basin record (Nowaczyk 1997). However, the intensity is lower than before the N–R transition and it decays again after a short time. The R–N transition at about 35 ka is accompanied again by extreme low values of relative palaeointensity, followed by a significant increase with a maximum at 30 ka. Field intensity breaks down again and the field vector reverses polarity at about 27 ka, the onset of the Mono Lake excursion. In contrast to the Laschamp excursion, which exhibits typical behaviour of a short polarity event, this time the vector swings back to the normal-polarity state at 25 ka without an intensity increase during the reversed state. At a third level (246 cm), a single sample exhibits a reversed ChRM inclination (Fig. 8). The two neighbouring samples (above and below) show a trend to shallow inclinations at high AF levels (Fig. 10). This sample interval is also characterized by very low relative palaeointensities such as for the Mono Lake excursion and the N–R and R–N transitions of the Laschamp polarity excursion (Fig. 10). Moreover, rock magnetic parameters around 246 cm do not deviate from the properties of intervals documenting the Mono Lake excursion and the Laschamp excursion (Fig. 4). We therefore conclude that both the documented negative inclination(s) and the low relative palaeointensity around 246 cm could be the expression of a very short geomagnetic excursion at about 22 ka. Although the core dates back to approximately 145 ka, no further geomagnetic excursion is documented. The absence of the Norwegian–Greenland Sea excursion (Bleil & Gard 1989) around 70 ka and the Blake excursion (Smith & Foster 1969) around 115 ka is discussed in the following sections.

The MDF_{NRM} record as an indicator of the stability of the NRM exhibits some pronounced lows, in some cases at about the same depth intervals (246, 325 and 380–415 cm) where negative ChRM inclinations were determined (Fig. 8). These lows (the upper three) are caused by more or less antiparallel vector components of different coercivity: a hard reversed component superimposed by a soft normal overprint (Fig. 9). The term 'median destructive field' is strictly speaking only defined for univectorial magnetizations. Therefore, we cannot interpret this record in terms of NRM stability. Instead, we use the MDF of the ARM (dotted line in Fig. 8) to check relative changes of magnetic stability, because the ARM is a univectorial magnetization and thus provides unbiased information about the coercivity spectrum. The pronounced lows are not present in the MDF_{ARM} record, which indicates that the documented directions are not artefacts but records of geomagnetic field behaviour. Three other broad lows at about 475 cm (approximately 80 ka), 545 cm (approximately 130 ka) and 590 cm (approximately 140 ka) do not coincide with recorded non-normal ChRM directions. However, based on the age model shown in Fig. 3, at least the first two corresponding ages listed in brackets coincide roughly with ages for the Norwegian–Greenland Sea excursion and the Blake excursion, respectively (Nowaczyk *et al.* 1994; Langereis *et al.* 1997). Moreover, directions during magnetization at high AF amplitudes move towards shallow inclinations (Fig. 10), but do reach a stable endpoint. They might thus possibly be interpreted as relicts of a reversed magnetization that is almost completely covered by a normal overprint and that cannot be removed with the AF technique.

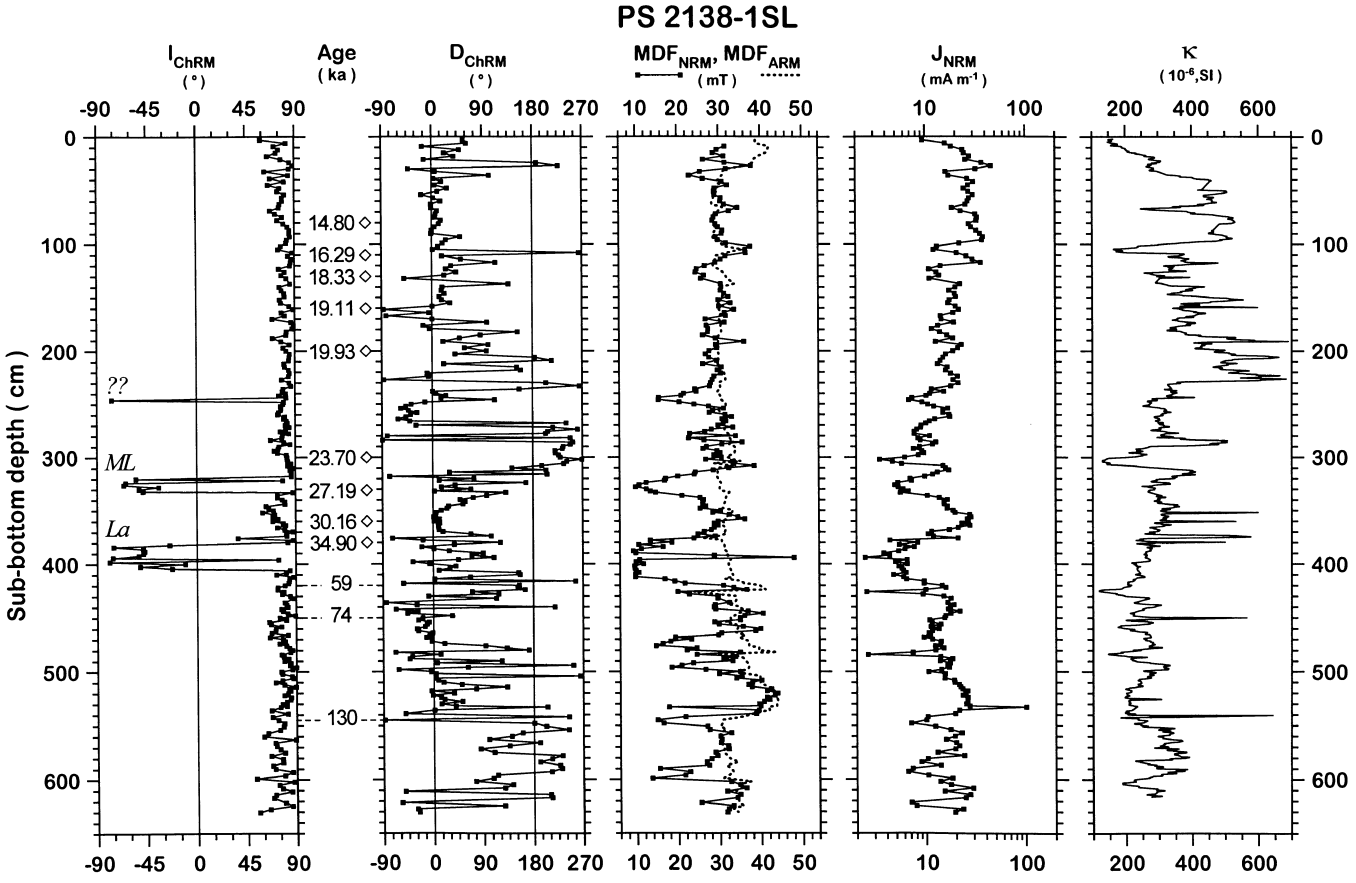

Figure 8. Palaeomagnetic results from core PS 2138–1 SL: inclination and declination of the characteristic remanent magnetization (I_{ChRM} and D_{ChRM}), calibrated AMS ^{14}C ages (open diamonds) and oxygen isotope stage boundaries (dashed lines), the median destructive field of the natural remanent magnetization (MDF_{NRM}, squares) and the anhysteretic remanent magnetization (MDF_{ARM}, dotted line), the NRM intensity (J_{NRM}) and the results from high-resolution logging of the magnetic susceptibility (κ). ML: Mono Lake excursion; La: Laschamp excursion.

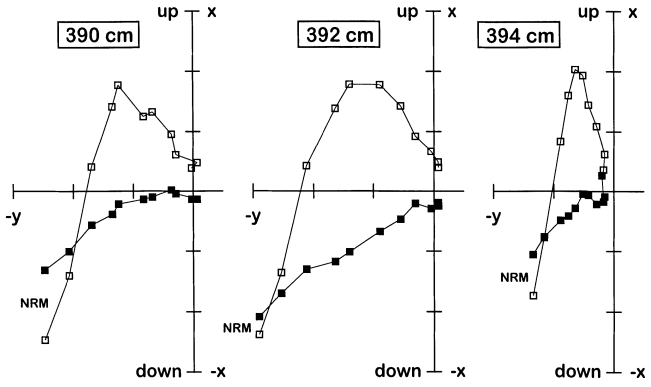

Figure 9. Zijderveld diagrams of three successive samples from the Laschamp excursion documented in core PS 2138–1 SL. Solid (open) symbols denote the horizontal (vertical) plane. Demagnetization steps are NRM, 5, 10, 15, 20, 30, 40, 50, 65, 80 and 100 mT.

CORRELATION TO OTHER RECORDS AND DISCUSSION

Considering current age models, a correlation between the magnetic susceptibility and ChRM inclination of PS 2138–1 SL and core PS 2212–3 KAL (Nowaczyk *et al.* 1994) from the Yermak Plateau (Fig. 1) is shown in Fig. 11. To account for the variable sedimentation rates in the two cores we used two different scalings within the corresponding depth axis. The chronology of PS 2212–3 KAL is based on calcareous nannofossil biostratigraphy (coccoliths) and correlation to another sediment core, PS 1533–3 SL, taken close to site PS 2212, which is dated by coccolith stratigraphy, oxygen isotope stratigraphy and ^{230}Th and ^{10}Be stratigraphy (Nowaczyk *et al.* 1994). Despite the different resolutions caused by different sedimentation rates (Fig. 3), as well as different logging methods (core PS 2212–3 KAL was scanned with the MS2F sensor with lower spatial resolution), the correlation of the two cores can be fine-tuned by means of magnetic susceptibility. A hiatus in PS 2212–3 KAL found by correlation with PS 1533–3 SL (Nowaczyk *et al.* 1994) can now be confirmed by correlation with core PS 2138–1 SL (two exclamation marks in Fig. 11). A second hiatus or at least strongly reduced sedimentation in the interval between the Mono Lake excursion and the Laschamp excursion in core PS 2212–3 KAL can possibly be recognized as well (two question marks in Fig. 11). With the new correlation, the unexpectedly high amount of reversed directions in this core is obviously the result of strongly variable sedimentation rates which could not be revealed with the rough depth–age model originally provided for this core (Fig. 3).

In both cores the Mono Lake excursion (ML) and the Laschamp excursion (La) are well documented. The possible excursion at 246 cm (22 ka, AMS ^{14}C calibration) in PS 2138–1 SL is not documented at site PS 2212, but this core provides

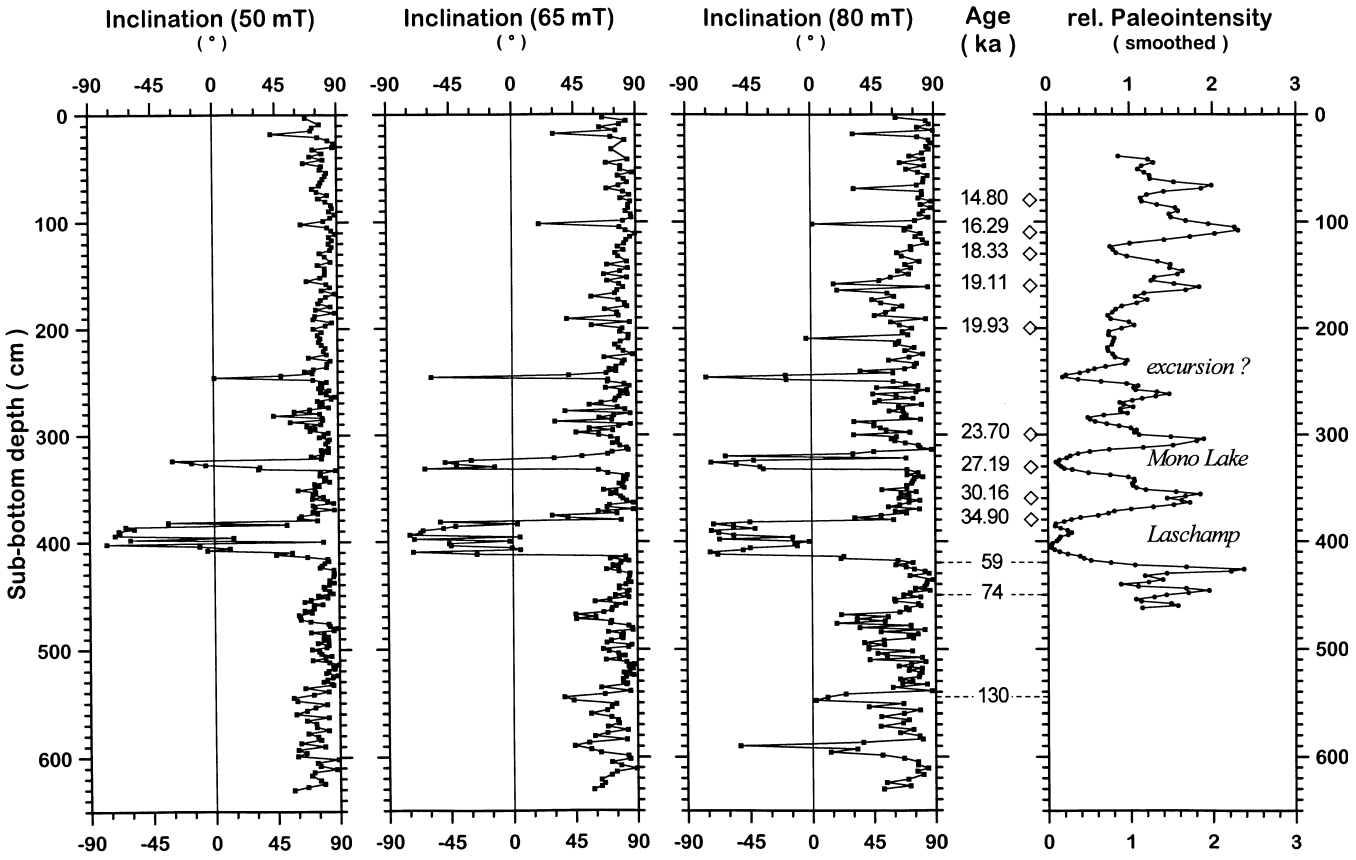

Figure 10. Directional behaviour of core PS 2138–1 SL as expressed by inclination versus depth and AF demagnetization level shown for steps with 50, 65, and 80 mT AF amplitude together with the palaeointensity estimate [J_{NRM}(50 mT)/J_{ARM}(50 mT)], smoothed with a three-point triangular window (*cf*. Fig. 6). Ages refer to calibrated AMS ^{14}C dates (open diamonds) and oxygen isotope stage boundaries (dashed lines). See also Fig. 2 and Table 1.

only a low temporal resolution for the corresponding time interval. Although the temporal resolution in both cores for stage 5 is equivalent, the Norwegian–Greenland Sea excursion (NGS) as well as the Blake excursion (Bl), which are documented by relatively long depth intervals of fully reversed directions in core PS 2212–3 KAL, are absent in core PS 2138–1 SL. Stage 5 sediments of the latter core are characterized by increased total organic carbon (TOC) contents of about 1 per cent, whereas other core sections have TOC contents of only 0.4 per cent, similar to TOC contents in stage 5 sediments (0.5 per cent) of core PS 2212–3 KAL (Voigt 1997).

Moreover, the interval where the Blake excursion could be expected by the correlation (490–510 cm) and its underlying sediments are characterized by strongly increased values of MDF_{ARM} and the κ_{ARM}/κ_{LF} ratio, indicating a reduced grain size of the magnetic carriers (magnetite). This could be an indicator of post-depositional, early diagenetic processes associated with dissolution of the original magnetic minerals and/or with long-term acquisition of a new chemical remanent magnetization (CRM), resulting in the loss of the original synsedimentary palaeomagnetic information such as described by Dekkers *et al.* (1994). Such types of sediments are suitable neither for relative palaeointensity estimations nor for the investigation of high-frequency directional changes of the geomagnetic field. Up to now, only very sparse geochemical information has been available for the Arctic Ocean sediments investigated. Comprehensive future studies, combining geochemical with rock magnetic methods (e.g. Passier *et al.* 1996), have to be performed in order to check the role of the TOC content and other geochemical properties of the sediment (e.g. sulphur) in the alteration of a synsedimentary magnetization in Arctic sediments.

Other cores from the Yermak Plateau area also show indications for geomagnetic excursions within stages 2 and 3 (Løvlie *et al.* 1986; Schneider *et al.* 1996). Only the data set for core PS 2213–6 of Schneider *et al.* (1996) includes a palaeointensity estimate, but the record is of low resolution, with only about 25 data points for the last $\approx$50 kyr and a relatively long data gap comprising approximately stages 4 and 5. Nevertheless, here again the Laschamp excursion is also characterized by a pronounced low in relative palaeointensity.

Using the age information provided for PS 2138–1 SL, we also performed a correlation based on relative palaeointensity variations to ODP site 983 (Fig. 12a) from the Gardar Drift (60.40°N, 23.64°W), investigated by Channell *et al.* (1997). The resulting age model is shown in Fig. 12(b). For the time interval 35–10 ka, about 3.5 m in length in PS 2138–1 SL, both records allow a detailed peak-to-peak correlation. For the older section from 80 to 35 ka, condensed in an interval of only 0.7 m in PS 2138–1 SL, only the major features of the palaeointensity record from ODP site 983 can be identified in the Arctic Ocean record. However, when plotted on a common time axis, the nearly perfect match between the two records becomes obvious (Fig. 13). Both relative palaeointensity

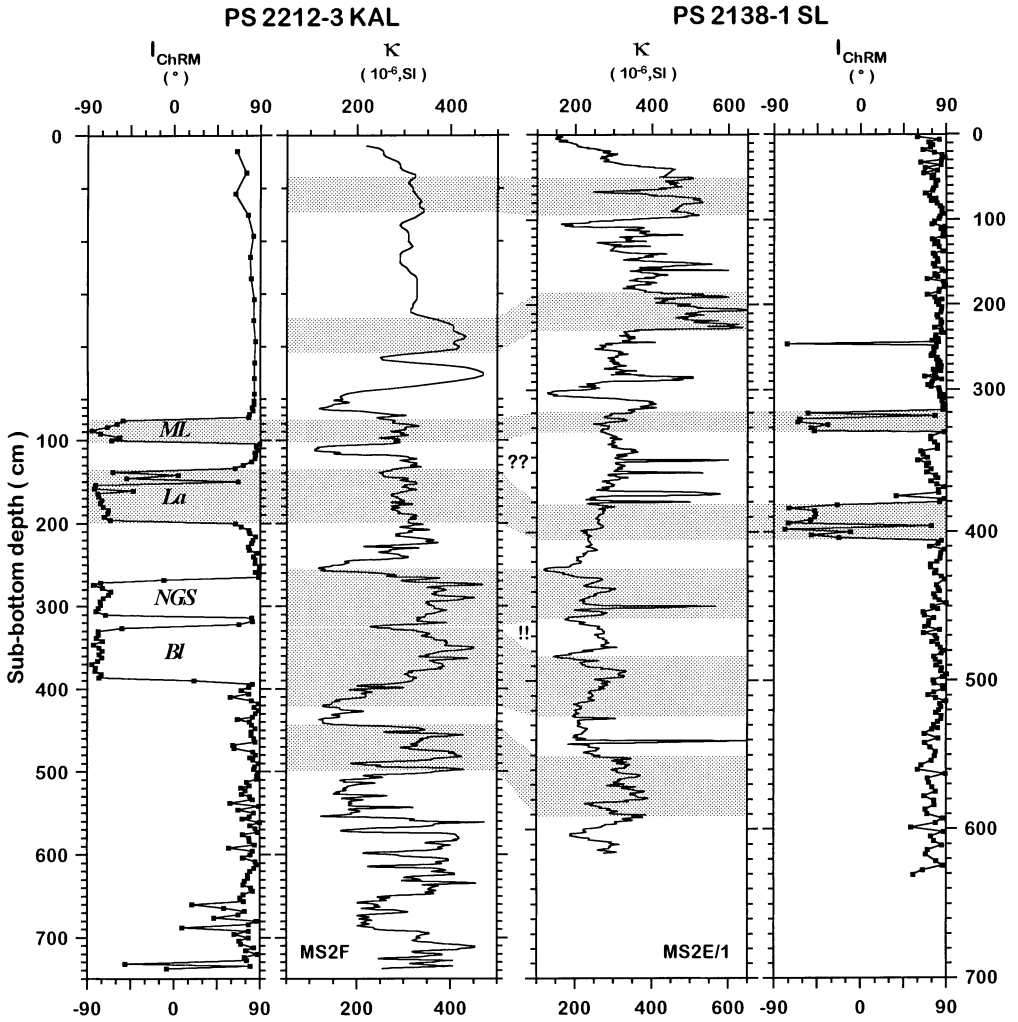

Figure 11. Correlation of PS 2138–1 SL to PS 2212–3 KAL from the Yermak Plateau by means of magnetic susceptibility (κ_{LF}) and ChRM inclination (I_{ChRM}). The two exclamation marks indicate the hiatus in PS 2212–3 KAL, already known from the investigation by Nowaczyk *et al.* (1994), and the two question marks indicate a further interval of at least significantly lower sedimentation rates in core PS 2212–3 KAL. MS2F and MS2E/1 denote the two different Bartington susceptibility logging sensors used for scanning the cores. ML: Mono Lake excursion; La: Laschamp excursion; NGS: Norwegian–Greenland Sea excursion; Bl: Blake excursion.

records are superimposed on the 'SINT800' stack of Guyodo & Valet (1999), together with its standard error range. When comparing the relative palaeointensity record from site PS 2138 to the ODP site 983 record as well as to the 'SINT800' stack, the most striking difference is the much higher dynamic range of the variations in the Arctic Ocean record. The 'SINT800' composite comprises 33 relative palaeointensity records, stacked by using the original age models of the data sets. This resulted in smoothing high-frequency features that were present in the individual records. Compared to ODP site 983, core PS 2138–1 SL has a much higher dynamic range. The Laschamp excursion has a very low relative palaeointensity, decreasing to 5 per cent of the average in the Arctic Ocean record, whereas the corresponding low in the North Atlantic record only decreases to 20 per cent of its average palaeointensity. Also, the differences at 25 ka (Mono Lake excursion) and at 19.5 ka (possible excursion in PS 2138–1 SL) are much more pronounced, 10 per cent in the Arctic Ocean record compared to 50–60 per cent in the North Atlantic record. In the time interval 15–30 ka, the sedimentation rate in PS 2138–1 SL is approximately 18 cm kyr^{-1}, almost twice as high as at site ODP 983, where it is 10–12 cm kyr^{-1}. Here the directional record shows only scattered but still positive inclinations for the time interval of the Mono Lake and Laschamp excursions. This might be an indication that here the palaeomagnetic signal, directional as well as intensity variations, has been smoothed during the remanence acquisition process, maybe as a result of lower sedimentation rates than at site PS 2138 in the Arctic Ocean.

All tie-points of the correlation (Fig. 12a shows only a subset) from PS 2138–1 SL to ODP 983 are plotted as crosses in Fig. 12(b), together with the original age model of PS 2138–1 SL (open diamonds) and the uncalibrated AMS ^{14}C ages (closed diamonds). Ages for ODP site 983 were derived from an oxygen isotope stratigraphy tuned to the SPECMAP reference curve (Imbrie *et al.* 1984), which is based on uncalibrated ^{14}C ages in the younger part. Differences in the ages derived from the correlation to ODP site 983 and ages derived directly from AMS ^{14}C determinations on PS 2138–1 SL (calibrated as well as uncalibrated) are in the range of only a few thousand years in the high-resolution interval from about 30 to 10 ka.

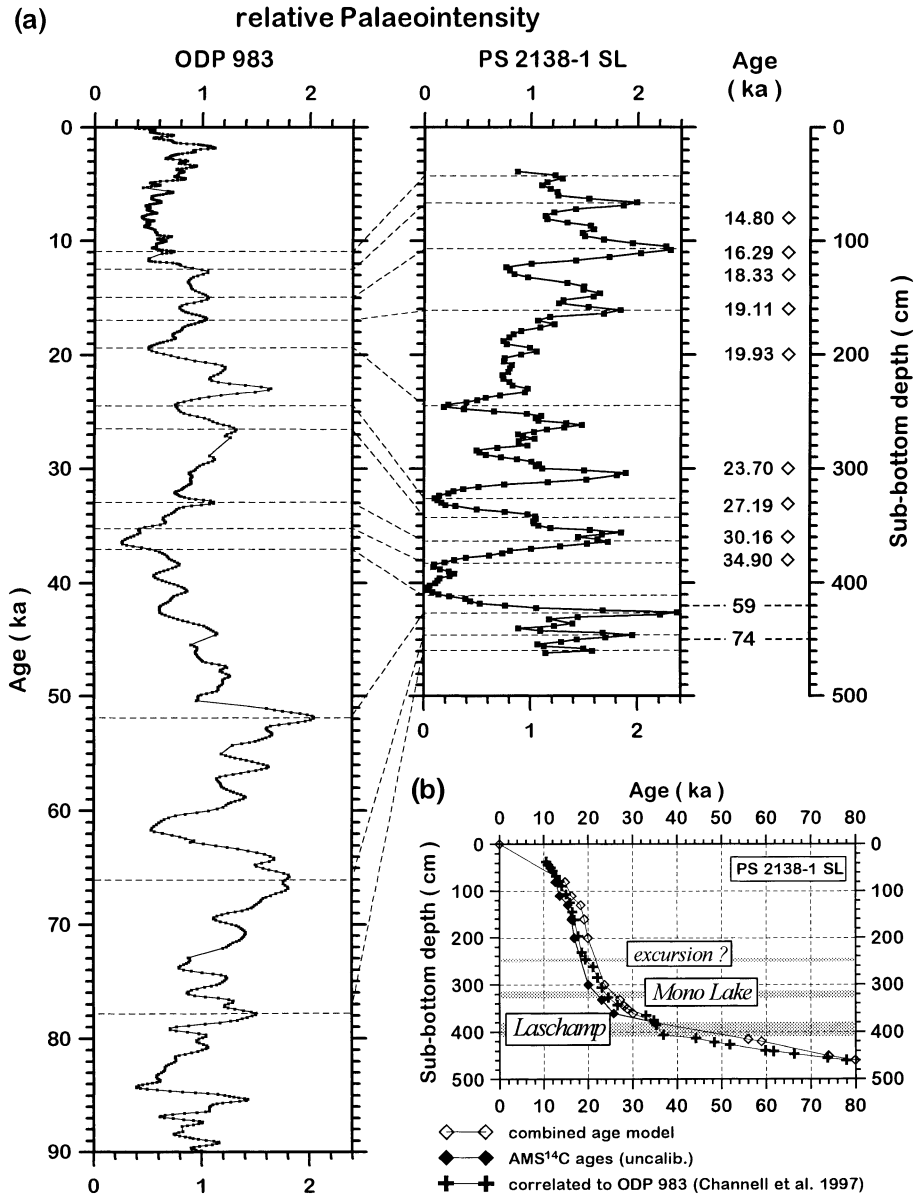

Figure 12. (a) Correlation of relative palaeointensity records from ODP site 983 (left) (after Channell *et al.* 1997) and core PS 2138–1 SL (right). Ages refer to calibrated AMS ^{14}C dates (open diamonds) and oxygen isotope stage boundaries (dashed lines). (b) Original age models of core PS 2138–1 SL for the time interval 0–80 ka and the new age model based on correlation to ODP site 983 (see also Fig. 2 and Table 1).

At 80 ka both models yield the same ages. Between 80 and 30 ka ages seem to differ significantly. However, because of the low sedimentation rates, slight shifts of age tie-points with respect to depth result in a large shift with respect to time. Since the stable isotope record from PS 2138–1 SL is not well defined in the time interval from 35 ka (380 cm = middle of stage 3) to 74 ka (450 cm = stage boundary 4/5), linear interpolation between the fixing points of the original age model would yield an unrealistically long duration for the Laschamp polarity excursion from 52 to 35 ka (Fig. 12b). The correlation of the palaeointensity record of PS 2138–1 SL to ODP site 983 re-dates the onset of the Laschamp to about 37 ka, but the low sedimentation rates still do not allow a precise age determination. However, an interval from 37 to 35 ka is in a better agreement with ages and durations for the Laschamp excursion as compiled by Nowaczyk *et al.* (1994) and with results from sediment cores taken at 73°N, where a high-resolution stable oxygen and carbon isotope stratigraphy supported by one AMS ^{14}C date yielded a duration of the Laschamp excursion from 37 to 33 ka (Nowaczyk & Antonow 1997).

The good correlation between core PS 2138–1 SL from 81.5°N and ODP site 983 from 60.4°N, more than 2000 km apart, provides evidence that the recorded relative palaeointensity variations at both sites are of at least regional if not global validity in the sense of real field intensity fluctuations. The associated directional variations documented in the Arctic Ocean record, as well as in other records of the Greenland Sea (Løvlie *et al.* 1986; Bleil & Gard 1989; Nowaczyk & Baumann 1992; Nowaczyk *et al.* 1994; Schneider *et al.* 1996; Nowaczyk & Antonow 1997; Völker *et al.* 1998; Nowaczyk & Frederichs 1999), indicate a strongly variable geomagnetic field, as discussed by Gubbins (1999), rather than a 'stable

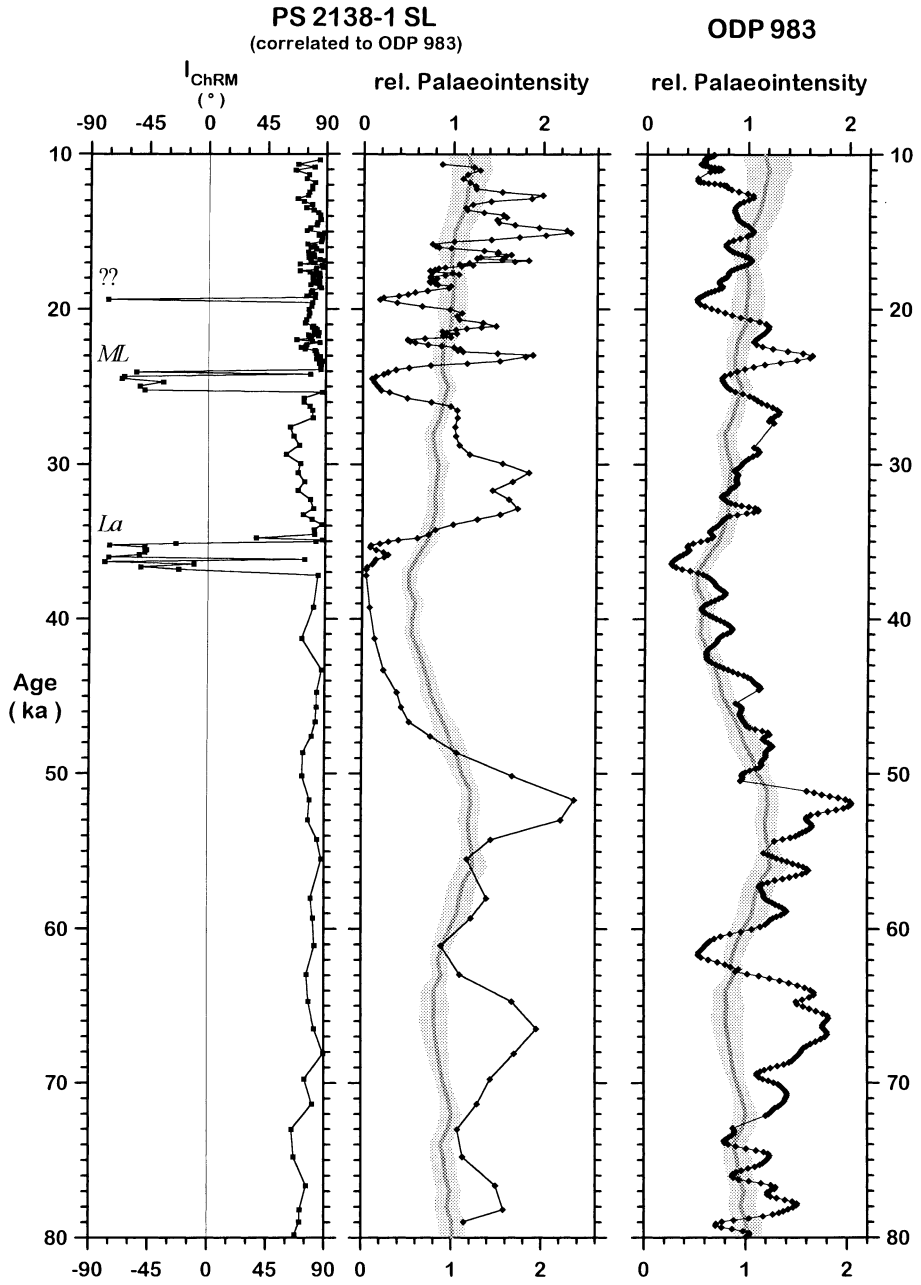

Figure 13. ChRM inclination (I_{ChRM}, left) and relative palaeointensity (middle) of PS 2138–1 SL after correlation with site ODP 983 (Channell *et al.* 1997; right). The grey curves and shaded areas indicate the 'SINT800' relative palaeointensity stack (Guyodo & Valet 1999) with its standard error range. ML: Mono Lake excursion; La: Laschamp excursion.

dipole configuration' as would be inferred from published geomagnetic polarity timescales (e.g. Cande & Kent 1995) that only reflect the changes in sign of the earth's dipole component. Gubbins (1999) discussed the role of the Earth's inner core as a stabilizing component in the geodynamo process. Gubbins argued that for a full reversal it is necessary, taking the Brunhes Chron as an example, for the reversed flux generated by convection within the outer core to be able to diffuse into the inner core, which needs about 3–5 kyr, in order to achieve a full reversal. If this is not successful, that is, convections in the outer core break down again before the associated reversed flux fully diffuses into the inner core, the geodynamo is forced back into its normal-polarity state again. The result is a short reversal excursion typically associated with low field intensity. The results presented in this paper strongly support this model.

A special problem of AMS ^{14}C dating of the Laschamp excursion arises from this geomagnetic feature itself. The directional changes of the Laschamp excursion are accompanied by a pronounced low in geomagnetic field intensity, determined with relative methods (Nowaczyk 1997; Völker *et al.* 1998; this study) as well as absolute methods (Massif Central, France: Barbetti & Flude 1979; Roperch *et al.* 1988; Chauvin *et al.* 1989; Skalamælifell, Iceland: Marshall *et al.* 1988; Levi *et al.* 1990). This results in a higher production of ^{14}C compared to times of a strong magnetic field and therefore apparently younger ^{14}C ages. The same is valid for the Mono Lake

Table 2. Ages of geomagnetic excursions found in core PS 2138–1 SL. The onset of the Laschamp event is not covered by AMS ^{14}C dating.

Geomagnetic excursion	Age		
	AMS ^{14}C uncalibrated	AMS ^{14}C calibrated	correlated to ODP 983
New excursion?	18	22	19.5
Mono Lake excursion	23.0–21.5	27.0–25.5	24.5–23.5
Laschamp excursion	??–35	??–35	37–35

excursion and the possible excursion at 18 ka (uncalibrated ^{14}C, Fig. 12b). Therefore, ^{14}C ages have to be calibrated by independent methods (e.g. Stuiver & Reimer 1993; Laj *et al.* 1996; Völker *et al.* 1998). So far, no really reliable calibration function for ages older than 12 kyr is available (Grootes, personal communication, 1999). Additionally, the most likely age range of the Laschamp, 40–35 ka based on K–Ar, ^{40}Ar/^{39}Ar, Thermoluminescence and ^{14}C (e.g. Hall & York 1978; Gillot *et al.* 1979), is close to the methodological limits of the AMS ^{14}C method (about 50 ka). However, to provide ages that can be compared to other calibrated records, we decided to use calibrated ages for discussing the results. For future (re-) calibration we have also listed the ages of the geomagnetic excursions based on uncalibrated AMS ^{14}C ages in Table 2.

CONCLUSIONS

The high-resolution palaeomagnetic investigation of core PS 2138–1 SL confirmed again the existence of the Mono Lake excursion and the Laschamp polarity excursion. Normalization of the NRM intensity after 50 mT with concentration-related rock magnetic parameters, low-field magnetic susceptibility, IRM and ARM (demagnetized with 50 mT) consistently yielded pronounced lows within the relative palaeointensity record associated with these excursions. Another low linked to at least one sample of negative ChRM inclination might give indications for an additional excursion at 22 ka (AMS ^{14}C, calibrated). Relative palaeointensity variations correlate well with a high-resolution record from the North Atlantic at 61.4°N, but the dynamic range of the amplitudes is much more pronounced in the Arctic Ocean record. The smaller dynamic range of documented relative palaeointensity variations and the absence of geomagnetic excursions in other records indicate that here the palaeomagnetic signal has already been smoothed during the remanence acquisition process. On the other hand, both the absence of geomagnetic excursions (the Norwegian–Greenland Sea and Blake excursions) and strongly deviating palaeointensity estimates in the Arctic Ocean record for stages 1 and 5 sediments with relatively low deposition rates can possibly be attributed to anomalous rock magnetic properties of the corresponding remanence carriers, obviously caused by early diagenetic processes.

ACKNOWLEDGMENTS

We thank the captain and crew of *R/V Polarstern* for their co-operation during expedition ARK VIII/2. G. Meyer, G. Traue, L. Schönicke, J.-M. Nadeau, and P. J. Grootes are greatly acknowledged for stable isotope analyses and AMS ^{14}C measurements. K. Teuber and U. Brandt helped during sampling and laboratory work in Potsdam. We would also like to thank Y. Guyodo and J. E. T. Channell for providing their palaeointensity data sets and Cor Langereis and an anonymous referee for their constructive comments on the manuscript.

REFERENCES

Barbetti, M. & Flude, K., 1979. Palaeomagnetic field strengths from sediments baked by lava flows of the Chaîne des Puys, France, *Nature,* **278,** 153–156.

Bard, E., Arnold, M. & Hamelin, B., 1992. Present status of the radiocarbon calibration of the late Pleistocene, 4th international Conference on Paleoceanography, GEOMAR, Kiel, Germany, *Res. Center Mar. Geosci. Rept,* **15,** 52–53.

Bleil, U. & Gard, G., 1989. Chronology and correlation of Quaternary magnetostratigraphy and nannofossil biostratigraphy in Norwegian-Greenland Sea sediments, *Geol. Rundschau,* **78,** 1173–1187.

Bloemendal, J., King, J.W., Hall, F.R. & Doh, S.J., 1992. Rock magnetism of Late Neogene and Pleistocene deep-sea sediments: relationship to sediment source, diagenetic processes, and sediment lithology, *J. geophys. Res.,* **97,** 4361–4375.

Bonhommet, N. & Babkine, J., 1967. Sur la présence d'aimantations inversées dans la Chaîne des Puys, *C. R. Acad. Sci. Paris,* **264,** 92–94.

Cande, S.C. & Kent, D.V., 1995. Revised calibration of the geomagnetic polarity timescale for the Late Cretaceous and Cenozoic, *J. geophys. Res.,* **100,** 6093–6095.

Champion, D.E., Lanphere, M.A. & Kuntz, M.A., 1988. Evidence for a new geomagnetic reversal from lava flows in Idaho: discussion of short polarity reversals in the Brunhes and the late Matuyama Polarity Chrons, *J. geophys. Res.,* **93B,** 11 667–11 680.

Channell, J.E.T., Hodell, D.A. & Lehman, B., 1997. Relative geomagnetic paleointensity and δ^{18}O at ODP Site 983 (Gardar Rift, North Atlantic) since 350 ka, *Earth planet. Sci. Lett.,* **153,** 103–118.

Chauvin, A., Duncan, R.A., Bonhommet, N. & Levi, S., 1989. Paleointensity of the earth's magnetic field and K-Ar Dating of the Louchadière volcanic flow (Central France), New evidence for the Laschamp excursion, *Geophys. Res. Lett.,* **16,** 1189–1192.

Denham, C.R. & Cox, A., 1971. Evidence that the Laschamp polarity event did not occur 13300–30400 years ago, *Earth planet. Sci. Lett.,* **13,** 181–190.

Dekkers, M.J., Langereis, C.G., Vriend, S.P., van Santvoort, P.J.M. & Lange, G.J., 1994. Fuzzy *c*-mean cluster analysis of early diagenetic effects on natural remanent magnetisation acquisition in a 1.1 Myr piston core from the Central Mediterranean, *Phys. Earth. planet. Inter.,* **85,** 155–171.

Gillot, P.Y., Labeyrie, J., Laj, C., Valladas, G., Guérin, G., Poupeau, G. & Delibrias, G., 1979. Age of the Laschamp paleomagnetic excursion revisited, *Earth planet. Sci. Lett.,* **42,** 444–450.

Gubbins, D., 1999. The distinction between geomagnetic excursions and reversals, *Geophys. J. Int.,* **137,** F1–F3.

Guyodo, Y. & Valet, J.-P., 1999. Global changes in intensity of the earth's magnetic field during the past 800 kyr, *Nature,* **399,** 249–252.

Hall, C.M. & York, D., 1978. K-Ar and ^{40}Ar/^{39}Ar age of the Laschamp geomagnetic polarity reversal, *Nature,* **274,** 462–464.

Hall, F.R. & King, J.W., 1989. Rock-magnetic stratigraphy of Site 645 (Baffin Bay) from ODP Leg 105, *Proc. ODP,* **105,** 653–665.

Imbrie, J. *et al.*, 1984. The orbital theory of Pleistocene climate: support from a revised chronology of the marine δ^{18}O record, in *Milankovitch and Climate,* Part 1, ed. Berger, A.L., 269–305, Reidel, Dordrecht.

King, J.W., Banerjee, S.K., Marvin, J. & Özdemir, Ö., 1982. A comparison of different magnetic methods for determining the relative grain size of magnetite in natural materials: some results from lake sediments, *Earth planet. Sci. Lett.,* **59,** 404–419.

Kirschvink, J.L., 1980. The least-squares line and plane and the analysis of palaeomagnetic data, *Geophys. J. R. astr, Soc.,* **62,** 699–718.

Knies, J., 1999. Late Quaternary paleoenvironment along the northern Barents and Kara seas continental margin, a multi parameter analysis, *PhD thesis,* Bremen University, Germany.

Laj, C., Mazaud, A. & Duplessy, J.-C., 1996. Geomagnetic intensity and ^{14}C abundance in the atmosphere and ocean during the past 50 kyr, *Geophys. Res. Lett.,* **23,** 2045–2048.

Langereis, C.G., de Dekkers, M.J., Lange, G.J., Paterne, M. & Santvoort, P.J.M., 1997. Magnetostratigraphy and astronomical calibration of the last 1.1 Myr from eastern Mediterranean piston core and dating of short events in the Brunhes, *Geophys. J. Int.,* **129,** 75–94.

Levi, S., Audunsson, H., Duncan, R.A., Kristjansson, L., Gillot, P.-Y. & Jacobsson, S.P., 1990. Late Pleistocene geomagnetic excursion in Icelandic lavas: confirmation of the Laschamp excursion, *Earth planet. Sci. Lett.,* **96,** 443–457.

Liddicoat, J.C. & Coe, R.S., 1979. Mono Lake geomagnetic excursion, *J. geophys. Res.,* **84,** 261–271.

Løvlie, R., 1989a. Paleomagnetic stratigraphy: a correlation method, *Quat. Int.,* **1,** 129–149.

Løvlie, R., 1989b. Palaeomagnetic excursions during the last interglacial/glacial cycle: a sysnthesis, *Quat. Int.,* **3/4,** 5–11.

Løvlie, R., Markussen, B., Sejrup, H.P. & Thiede, J., 1986. Magnetostratigraphy in three Arctic Ocean sediment cores; arguments for geomagnetic excursions within oxygen-isotope stage 2–3, *Phys. Earth planet. Inter.,* **43,** 173–184.

Lund, S.P., Acton, G., Hastedt, M. & Williams, T., 1998. Geomagnetic field excursions occurred often during the last million years, *EOS, Trans. Am. geophys. Un.,* **79,** 178–179.

Marshall, M., Chauvin, A. & Bonhommet, N., 1988. Preliminary paleointensity measurements and detailed magnetic analysis of basalts from the Skalamaelifell excursion, southwest Iceland, *J. geophys. Res.,* **93,** 11 681–11 698.

Nowaczyk, N.R., 1997. High-resolution magnetostratigrahy of four sediment cores from the Greenland Sea—II. Rock magnetic and palaeointensity data, *Geophys. J. Int.,* **131,** 325–334.

Nowaczyk, N.R. & Antonow, M., 1997. High-resolution magneto-stratigraphy of four sediment cores from the Greenland Sea—I. Identification of the Mono Lake excursion, Laschamp and Biwa I/ Jamaica geomagnetic polarity events, *Geophys. J. Int.,* **131,** 310–324.

Nowaczyk, N.R. & Baumann, M., 1992. Combined high-resolution magnetostratigraphy and nannofossil biostratigraphy for late Quaternary Arctic Ocean sediments, *Deep Sea Res.,* **39,** 567–601.

Nowaczyk, N.R. & Frederichs, T.W., 1999. Geomagnetic events and relative paleointensity variations during the last 300 ka as recorded in Kolbeinsey Ridge sediments, Iceland Sea—indication for a strongly variable geomagnetic field, *Int. J. Earth Sci.,* **88,** 116–131.

Nowaczyk, N.R., Frederichs, T.W., Eisenhauer, A. & Gard, G., 1994. Magnetostratigraphic data from late Quaternary sediments from the Yermak Plateau, Arctic Ocean: evidence for four geomagnetic polarity events within the last 170 Ka of the Brunhes Chron, *Geophys. J. Int.,* **117,** 453–471.

Passier, H.F., Middelburg, J.J., van Os, B.J.H. & Lange, G.J., 1996. Diagenetic pyritisation under eastern Mediterranean sapropels caused by downward sulphide diffusion, *Geochim. Cosmochim. Acta,* **50,** 751–763.

Roberts, A.P., Lehman, B., Weeks, R.J., Verosub, K.L. & Laj, C., 1997. Relative paleointensity of the geomagnetic field over the last 200 000 years from the ODP Sites 883 and 884, North Pacific Ocean, *Earth planet. Sci. Lett.,* **152,** 11–23.

Roperch, P., Bonhommet, N. & Levi, S., 1988. Paleointensity of the earth's magnetic field during the Laschamp excursion and its geomagnetic implications, *Earth planet. Sci. Lett.,* **88,** 209–219.

Schneider, D.A., Backman, J.M.F., Curry, W.B. & Possnert, G., 1996. Paleomagnetic constraints on sedimentation rates in the eastern Arctic Ocean, *Quat. Res.,* **46,** 62–71.

Smith, J.D. & Foster, J.H., 1969. Geomagnetic reversal in Brunhes normal polarity epoch, *Science,* **163,** 565–567.

Stuiver, M. & Reimer, P.J., 1993. Extended ^{14}C data base and revised CALIB 3.0 ^{14}C age calibration program, *Radiocarbon,* **35,** 215–230.

Tauxe, L., 1993. Sedimentary records of relative paleointensity of the geomagnetic field: theory and practice, *Rev. Geophys.,* **31,** 319–354.

Tauxe, L. & Valet, J.-P., 1989. Relative paleointensity of the earth's magnetic field from marine sedimentary records: a global perspective, *Phys. Earth planet. Inter.,* **56,** 59–68.

Valet, J.-P. & Meynadier, L., 1993. Geomagnetic field intensity and reversals during the past four million years, *Nature,* **366,** 234–238.

Voigt, C., 1997. Regional and temporal variations of mineral assemblages in Arctic Ocean sediments as climatic indicator during glacial/interglacial changes, *PhD thesis,* Bremen University, Germany.

Völker, A.H.L., Sarnthein, M., Grootes, P.M., Erlenkeuser, H., Laj, C., Mazaud, A., Nadeau, M.-J. & Schleicher, M., 1998. Correlation of marine ^{14}C ages from the Nordic Seas with the GISP2 isotope record: implications for ^{14}C calibration beyond 25 ka, *Radiocarbon,* **40,** 517–534.

Weeks, R.J., Laj, C., Endignoux, L., Mazaud, A., Labeyrie, L., Roberts, A.P., Kissel, C. & Blanchard, E., 1995. Normalised natural remanent magnetisation intensity during the last 240 000 years in piston cores from the central North Atlantic Ocean: geomagnetic field intensity or environmental signal?, *Phys. Earth planet. Inter.,* **87,** 213–229.